ISSN 1392-2114 ULTRAGARSAS (ULTRASOUND), Vol. 65, No. 2, 2010.

Investigation of ultrasonic array

R. Kažys, L. Kairiūkštis

Ultrasound Institute,Kaunas University of Technology

Studentų 50, 51368 Kaunas, LITHUANIA, Phone: +370 37 351162, Fax. +370 37 451489,

E-mail: ulab@.ktu.lt.

Abstract

This paper explores the data collection method for the ultrasonic array which can drastically decrease the scanning time, because the minimum excitation-reception sequences were used for reconstruction of the coordinates of the defects. The described data collection and processing method do not use classical phased array possibilities such as beam steering and focusing, but can reconstruct the object under the test for all physically possible deeps and angles. Mentioned approach was modeled with the ultrasonic arrays which are used in non-destructive testing, but basic principles of it can be employed by other applications or industries where array are used.
Keywords: phased arrays, simulations, ultrasonic field, scanning algorithm, defect location.

Introduction

Arrays are widely used in radar, sonar applications, medical, seismic systems and non-destructive testing for a long time. The main advantage of the phased arrays to compare to monolithic transducers is their ability to steer and focus the ultrasonic beam to any point of interest within limits which are governed by transducer properties such as size of the individual elements, active aperture of the transducers, geometrical shape and others.

The simplest case of the phased array is linear (1D) array where the beam can be steered and focused in one plane. The more complicated are matrix or 2D arrays which can manipulate the beam it two planes. Cylindrical arrays are not so often met. One of the major advantages of the cylindrical array is that the beam can reach any arbitrary point around the probe, so such arrays are very practical for investigation the objects with an axial geometry. The main shortcoming of such arrays is limited focusing possibility due to cylindrical geometry of arrays. They were investigated in the previous studies of the focusing possibilities of cylindrical and convex arrays [1].

The beam steering and focusing by a phased array is implemented with different time delays applied to the individual element of the array. It is called the delay laws. By applying different delays laws we can obtain different scan methods: a) sector scan (sweeping the beam only); b) directional and deep focusing (we can sweep the focused beam in selected deep); c) several deep focusing (the beam is focused at several distances from the probe without sweeping); d) single point focusing (the beam can be focused to any arbitrary point of interest within the focusing possibilities of the array) e) if we will apply null delay law to the defined number of the arrays elements we can get a single transducer case with a variable aperture.

So using ultrasonic arrays we can observe object from one position and get more detailed view to compare to a monolithic transducer. Variable focusing increases the resolution of inspection, but it is always time consuming to apply the *n* number of different delays laws to focus to any arbitrary point in the tested space. To minimize the number of different delays laws we should choose the necessary inspection resolution. The resolution determines the size of the detectable defect and the number of shots to be applied to the phased array. So the total time for inspecting the object will be calculated by summing times of the transducer for emitting ultrasonic waves toward an examination points, and times which are needed to receive waves from these points.

The aim of this investigation is development of the scanning and processing method for the array which guarantees that the coordinates of the defect can be estimated during shorter inspection time, what allows to use such system in the real time non destructive testing. The simplest electronic system can be used for implementing such algorithm because beam steering and focusing is not used in the method described below. The probe is not moved along the object under test, but all area of inspection is covered by exiting the elements in the row.

The scanning sequence

To make scanning algorithm suitable for online inspection we should minimize the number of shots. To get steered or focused beam phased arrays employs emitting and receiving delays laws which can be different or equal, but in our case we did not use delay laws and we collected all necessary data in four steps in 4 elements array case and in eight steps in 8 elements array case.

To investigate the data collection and processing algorithm we selected linear array (Fig.1). The defect can be in arbitrary position in the tested media, so to test the performance of the method we moved the defects in diferent positions.

Distances or paths Z_n to the defects from the centers of the phased array n^{th} element are given by:

$$Z_n = \sqrt{Z_d^2 + \left[H_p + (n-1)dx\right]^2}\,, \qquad (1)$$

$$Z_{n-1} = \sqrt{Z_d^2 + \left[H_p + (n-2)dx\right]^2}\,, \qquad (2)$$

The time delay between two neighbouring elements can be calculated:

$$\Delta t_n = \frac{Z_n - Z_{n-1}}{c}\ , \qquad (3)$$

The information about the distances Z_n is used to reconstruct image from the travel time to the individual transducer element. The superimposition of the signals received by different elements is done taking into account time delays Δt_n between neighbouring elements.

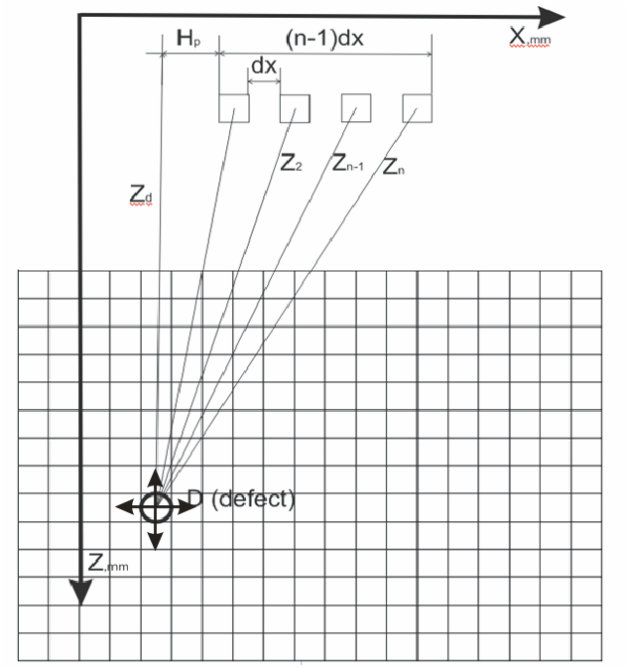

Fig.1. **Object under the test**

The data collection sequence for four elements linear sampling array is described by A. Bulavinov et all. [2], but for data processing we used only four signals (four element array case) instead of using sixteen. The used in computation signals were gotten by exiting all elements in a row and receiving signal by the same element which emits (highlighted in the table 1).

The scanning sequence in Table 1 can be employed by the array of unlimited number of the elements. As well, to empower more acoustical energy we can subdivide phased array into groups with certain numbers of elements and apply the same emitting-receiving matrix like we use in four element case. For example we can subdivide 16 elements array into 4 virtual element arrays where each element will be formed from 4 elements which will act as one. To work in the extreme near field is better to use the smaller active aperture or smaller elements with shorter near field, because the size of the active aperture is governed by the near field and can be varied in the algorithm.

To implement scanning sequence the array of 4 rectangular elements was placed in the coupling medium - water. The length of element – 10 mm and the width – 1.5 mm. The simulations of the wave front of individual array elements were calculated using the toolbox Ultrasim for Mathlab [3].

Table 1. **The scanning sequence matrix for 4 elements array. Only highlighted signals used in data processing.**

Sequence	Element number which emits	Element number which receives
1st	1st	1st
		2nd
		3rd
		4th
2nd	2nd	1st
		2nd
		3rd
		4th
3rd	3rd	1st
		2nd
		3rd
		4th
4th	4th	1st
		2nd
		3rd
		4th

Responses from defects were collected using CIVA software [4]. Both software vendors use the Huygens' principle in computations, which states that wave interactions can be analyzed by summing the phases and amplitudes by a number of spherically radiating simple sources. The pressure at a given distance from the source is computed [3]:

$$p(r,t) = \left(\frac{p_0 a}{r}\right)^{1/2} \exp[j(\omega t - kr) - \alpha r]\ , \qquad (4)$$

where p_0 is the initial pressure, a is the constant, α is the attenuation coefficient and r is the radial distance from the source. The each element of the array was subdivided into number of point sources which vibrate in the same phase, so the element width and length are taken into account.

By emitting acoustical energy from the n-th element we can cover different areas of the object under the test and we will get reflections which will vary in amplitude and time from the defects placed in arbitrary positions, because the wave fronts of individual phased array elements are shifted along x axis. The two curves in pictures (Fig.2-5) show the wave front boundary at -6 dB level.

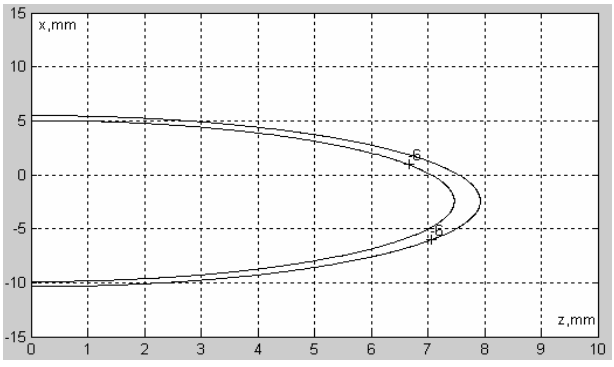

Fig.2. **Wave front at -6 dB level in x0z plane while emit and receive 1st element at time moment t=5 μs**

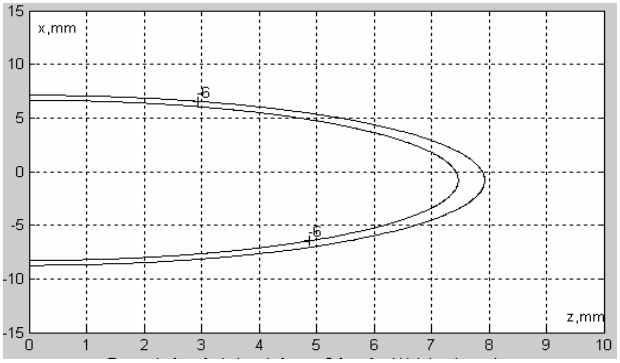

Fig.3. **Wave front at -6 dB level in x0z plane while emit and receive 2nd element at time moment t=5 µs**

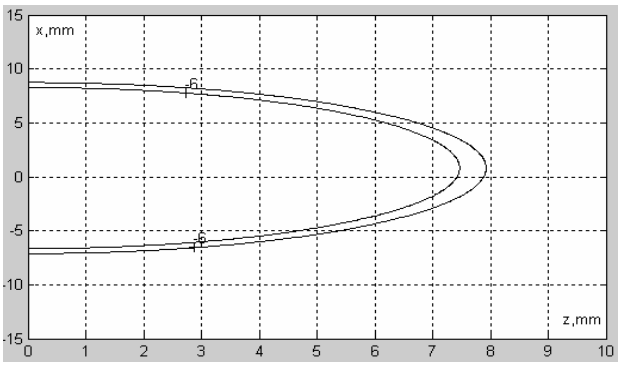

Fig.4. **Wave front at -6 dB level in x0z plane while emit and receive 3rd element at time moment t=5 µs**

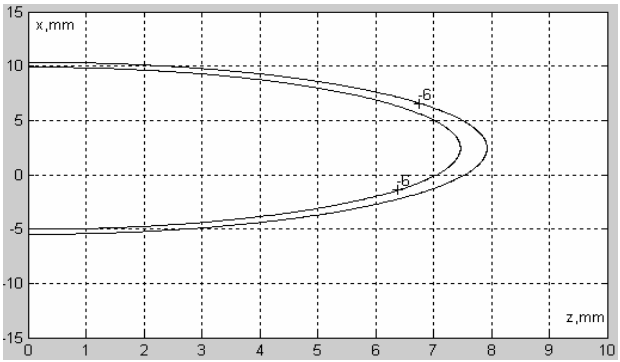

Fig.5. **Wave front at -6 dB level in x0z plane while emit and receive 4th element at time moment t=5 µs**

As well the collected signals can be viewed at different time lags – sampled. By sampling signals at different time instants time (t_1, t_2, ..., t_n) we can get information about the wave front at different distances (z_1, z_2, ..., z_n, z_{n+1}) from the probe. This helps us to determine the position of the defect along z axis.

When a scanning sequence is finished and data collection matrix (Table 2) is filled it is possible to reconstruct the image for all physically possible angles of incidence like in the sector or multi focusing scanning case.

The data processing principle

After performing scanning sequence we should process the obtained data. We will analyze 2 D case, so the chosen plane is $x0z$. After n-th element sends the signal all elements register time of flight of the received signal with the value of amplitude which is time related or sampled in the time domain (Table 2). The value of amplitude which is time related is used to determine if the time of flight will be taken into calculation or not.

Table 2. **The data needed for reconstruction**

	Time t_1, µs				Time t_2, µs				Time t_n, µs			
	Amplitude, dB				Amplitude, dB				Amplitude, dB			
z_1	x_1	x_2	…	x_n	x_1	x_2	…	x_n	x_1	x_2	…	x_n
z_2	x_1	x_2	…	x_n	x_1	x_2	…	x_n	x_1	x_2	…	x_n
…	…	…	…	…	…	…	…	…	…	…	…	…
z_n	x_1	x_2	…	x_n	x_1	x_2	…	x_n	x_1	x_2	…	x_n
z_{n+1}	x_1	x_2	…	x_n	x_1	x_2	…	x_n	x_1	x_2	…	x_n

Reconstruction of the defect view is done in two steps. First, we irradiate the object under the test according to the data the scanning sequence matrix (Table 1). So for four element array it is done in four steps. In our case all four elements operate in a pulse-echo mode, so each element sends and receives the signal from a reflector or defect.

As soon data are collected we can start processing of the A-scans. The collected signals can be viewed at different time lags. By comparing the time of flight we are able to determine the position of the defect along x axis. At this step we can reconstruct the image for arbitrary deep within limits by scaling the signal in the time axis.

To reconstruct defect coordinates we shall use the Kirchhoff migration technique, which is known from the field of seismic investigations [5]. According to the migration technique the location of a circular wave front at the time t can be found:

$$c^2t^2 = (x - x_0)^2 + (z - z_0)^2 \qquad (5)$$

where c is a speed of sound in media, t is the travel time from emitter to reflector (defect). Lets say that the array element (receiver) is at the position (z_0, x_0) where z_0= 0 and coordinate x_0 varies depending on a array elements center position. The z is equivalent to the radius of the circle:

$$z = \sqrt{c^2t^2 - (x_i - x_0)^2} \qquad (6)$$

The Eq.6 will be used for drawing circles where intersection of the circles arc will show the defect position.

Modeling

For testing of the proposed data collection and processing algorithm the 4 elements (Fig.6) and 8 elements ultrasonic arrays were selected. In both cases the size of individual elements and pitch are the same.

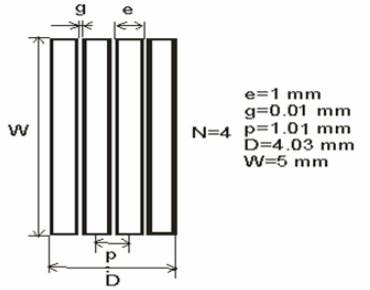

Fig 6. **Ultrasonic array with dimensions, where D – active aperture, g – interelement spacing, p – pitch, e – element width, W – passive aperture**

The probe was placed in a coupling media – water (c = 1483 m/s), so that coordinates of the center of the active aperture are z=0 mm and the x =25mm (Fig.7). The coordinates x_0 which describes positions of the centers of the active elements are following:

Table 3. **The *x* coordinates of the centers of array elements**

x_0,mm			
1 element	2 element	3 element	4 element
23.485	24.495	25.505	26.515

These positions define the scanning step along x axis which is equal to the pitch of array. We can tell that the resolution will increase as we will minimize the step, but has limits governed by the size of elements used in array.

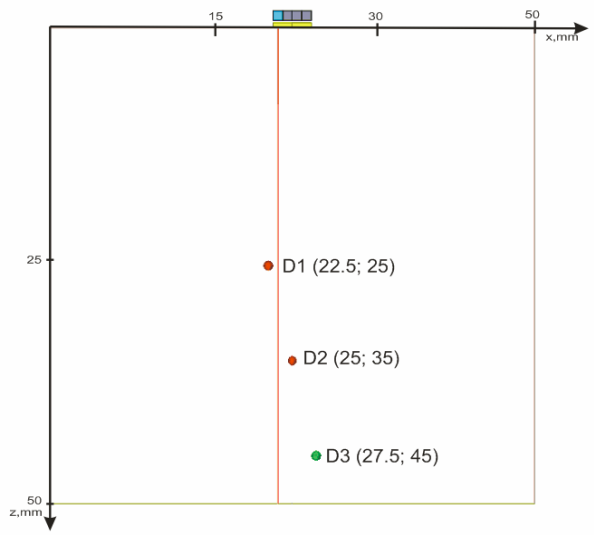

Fig 7. **Modeling setup, where the center of the array passive aperture is set to y=0 mm and the center coordinates of the defects D1, D2, D3 in y direction are set to 0 mm**

The 3 spherical stainless steel defects with the diameter D1=D2=D3=1 mm were placed in water at positions depicted in Fig.7. Elements of the array were exited by the gausian signal at the center frequency of 5 MHz (Fig.8).

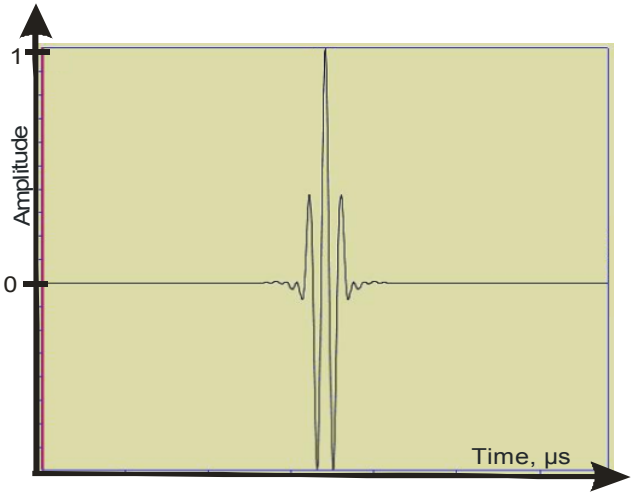

Fig 8. **Exitation signal at the center frequency 5 MHz used in simulation**.

The reflections from defects for each scanning sequence were collected as A-scan's from which the times of flight and amplitude were collected (Table 4).

Table 4. **Data collected during 4 elements array simulation**

Sequence	Coordinates of the defect (x,z)	Time of flight, μs	Amplitude, dB
1 defect			
1-1	22.5;25	33.07	0
2-2		33.15	-1.8
3-3		33.29	-4.7
4-4		33.47	-9.1
2 defect			
1-1	25;35	46.56	-3.1
2-2		46.52	-2.5
3-3		46.52	-2.5
4-4		46.56	-3.1
3 defect			
1-1	27.5;45	60.24	-9
2-2		60.13	-7.4
3-3		60.06	-6.5
4-4		60.01	-5.8

While distances from array elements to the reflector are different, we get reflected signals which values of amplitude and time of flights differ (Fig. 9, 10).

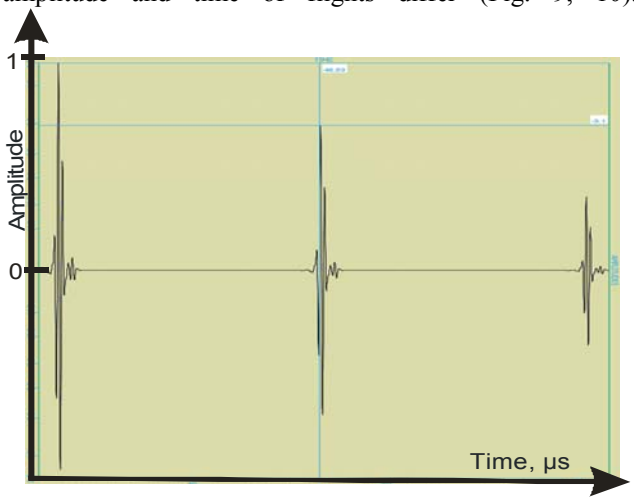

Fig.9. **A-scan when 1st element sends and 1st element receives**

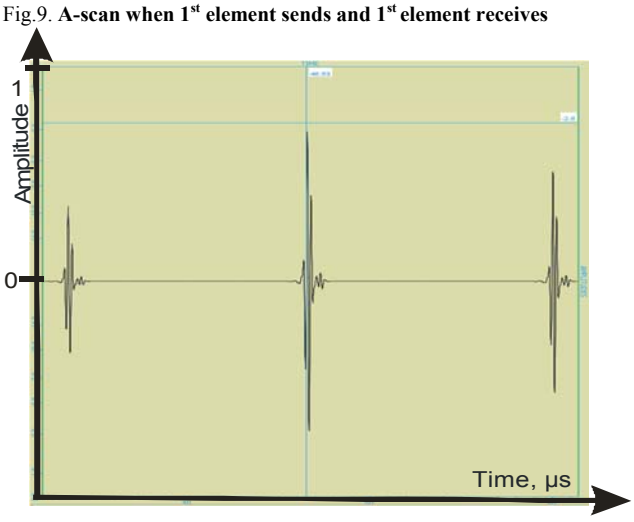

Fig.10. **A-scan when 4th element sends and 4th element receives**

After collection of the time of flights we solve Eq.2 and to draw circles for each scanning sequence, which define the center and radius of the circle. The intersection of the different circle arcs shows the position of the defect in (*x,z*) domain (Fig.11-15).

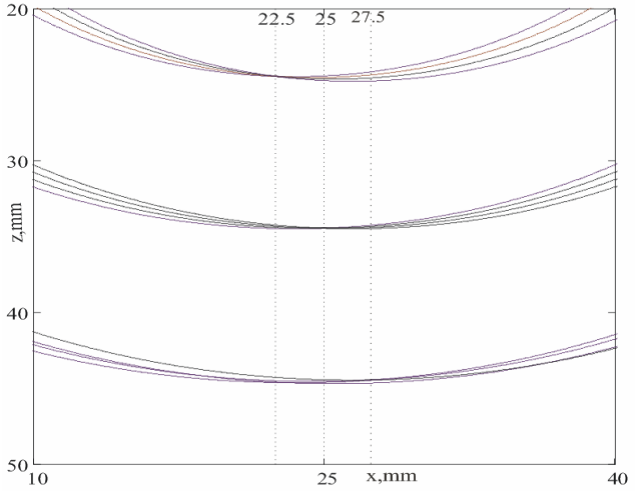

Fig. 11.**Superposition of four circles in *x,z* domain shows the coordinates of D1, D2, D3 defect (four element element array case)**

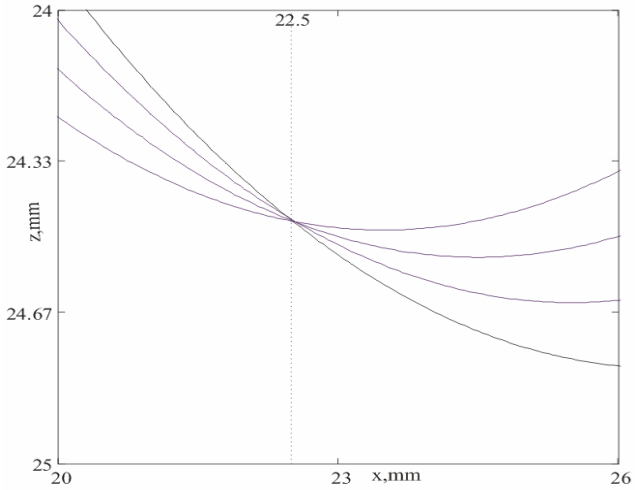

Fig. 12. **Expanded view of superposition of circles in *x,z* domain shows the coordinates of D1 defect which is placed at *x*=22.5 mm and *z* =25 mm. (four element element array case)**

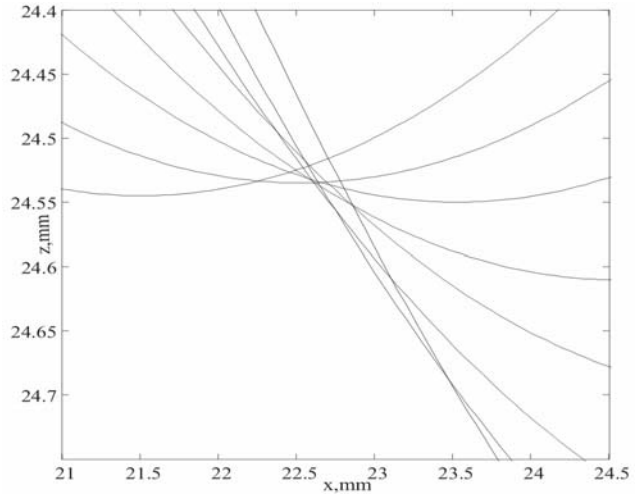

Fig. 13.**Superposition of circles in *x,z* domain shows the coordinates of D1 defect while 8 element array for simulation was used**

The intersections of the circles can be marked as the points (Fig. 14). After approximation of these points we can draw a curve which represents the upper part of the spherical defect.

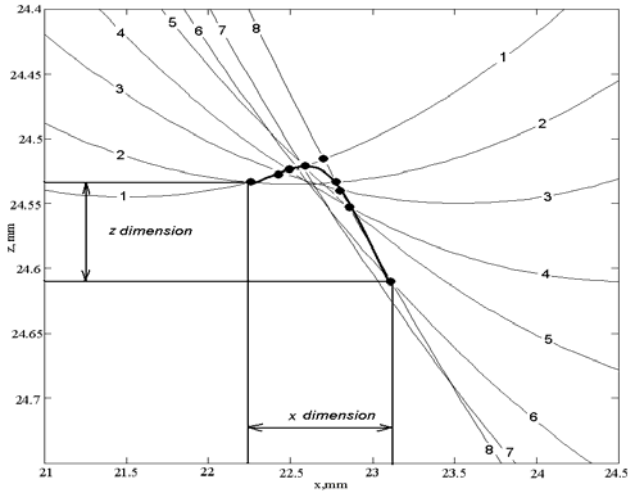

Fig. 14. **Expanded view of the superposition of circles in *x,z* domain shows the coordinates of D1 defect while 8 element array for simulation was used**

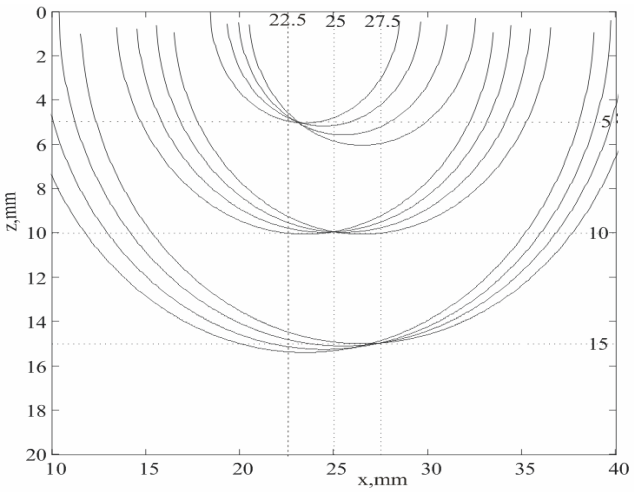

Fig. 15. **Superposition of four circles in *x,z* domain shows the coordinates of D1, D2, D3 defect (four element element array case). Defects are placed at the following distances from the probe : 5 mm, 10 mm, 15mm.**

Conclusions

The scanning sequence described above is useful in time consuming approach. This data collection and processing method for arrays allows reconstructing image for all physically possible angles of incidence without using beam focusing and steering. The proposed method works on 4 element arrays, but the increasing number of elements in array will increase resolution while we will get more intersections of the arcs of circles, so the curve which is drawn on top of intersections will approximate the position of a defect better. The method was validated while defects were placed at different distances from the probe.

References

1. **Kažys R., Kairiūkštis L.** Investigation of focusing possibilities of convex and cylindrical phased arrays. ISSN 1392-2114 Ultragarsas (Ultrasound). 2008. Vol. 63. No.4. P. 46-51.

1. **Bulavinov A., Pinchuk R., Pudovikov S., Reddy K. M, Walte F.** Industrial aplication of real-time 3D imaging by sampling phased array.

   http://i-deal-technologies.com/files/pdf/06.%20Industrial%20Application%20of%203D%20Imaging%20by%20Sampling%20Phased%20Array.pdf

2. Ultrasim toolbox home page http://heim.ifi.uio.no/~ultrasim/

3. CIVA software home page http://www-civa.cea.fr/

4. **Margrave G. F.**. Numerical methods of exploration seismology with algorithms in Matlab.

   http://www.crewes.org/ResearchLinks/FreeSoftware/EduSoftware/NMES_Margrave.pdf

R. Kažys, L. Kairiūkštis

Ultragarsinės gardelės kompleksinio skenavimo metodo tyrimas

Reziumė

Aprašytasis ultragarsinės gardelės duomenų surinkimo ir apdorojimo principas leidžia sumažinti skenavimo laiką ir gali būti panaudojamas įvairių geometrinių formų ultragarsinių gardelių darbui optimizuoti. Minėtasis principas leidžia be fokusavimo ir kampinio skenavimo atkurti tiriamojo objekto vaizdą esant skirtingiems objekto apspinduliavimo kampams ir gyliui.

Pateikta spaudai 2010 06 21

DOI: 10.5755/j01.u.65.2.17149